



## Semimonthly oscillation observed in the start time of equatorial Spread-F

Igo Paulino<sup>1</sup>, Ana Roberta Paulino<sup>2</sup>, Ricardo Yvan de la Cruz Cueva<sup>3</sup>, Ebenezer Agyei-Yeboah<sup>4</sup>, Ricardo Arlen Buriti<sup>1</sup>, Hisao Takahashi<sup>5</sup>, Cristiano Max Wrasse<sup>5</sup>, and Amauri Fragoso de Medeiros<sup>1</sup>

<sup>1</sup>Unidade Acadêmica de Física, Universidade Federal de Campina Grande, Campina Grande, Brazil

<sup>2</sup>Departamento de Física, Universidade Estadual da Paraíba, Campina Grande, Brazil

<sup>3</sup>Departamento de Física, Universidade Estadual do Maranhão, São Luís, Brazil

<sup>4</sup>Instituto de Pesquisa e Desenvolvimento, Universidade do Vale do Paraíba, São José dos Campos, Brazil

<sup>5</sup>Divisão de Aeronomia, Instituto Nacional de Pesquisas Espaciais, São José dos Campos, Brazil

**Correspondence:** Igo Paulino ([igo.paulino@df.ufcg.edu.br](mailto:igo.paulino@df.ufcg.edu.br))

### Abstract.

Using data from airglow an all sky imager and a coherent backscatter radar deployed at São João do Cariri (7.4°S, 36.5°W) and São Luís (2.6°S, 44.2°W), respectively, the start time of equatorial Spread-F were studied. Data from a period of over 10 years was investigated from 2000 to 2010. The semimonthly oscillations were clearly revealed in the start time of plasma bubbles from Oi6300 airglow images during three periods (September 2003, September-October 2005, November 2005 and January 2008). Since the airglow measurements are not continuous in time, more than one cycle of oscillation in the start time of plasma bubbles cannot be observed from these data. Thus, coherent backscatter radar data appeared as an alternative to investigate the start time of the ionospheric irregularities. Semimonthly oscillation were observed in the start time of plumes (November 2005) and bottom type Spread-F (November 2008) with at least one complete cycle. Technical/climate issues did not allowed to observe the semimonthly oscillations simultaneously by the two instruments, but from September to December 2005 there was a predominance of this spread-F start time oscillation over Brazil. The presence of this oscillation certainly contribute to the day-to-day variability of spread-F.

**Keywords:** Spread-F, Plasma bubble, Semimonthly oscillation, Plumes.

### 1 Introduction

Equatorial plasma bubbles (EPBs) appear in the bottom side of the F-region in the equatorial ionosphere when there is an unstable F-layer. It generally occurs after the pre-reversal enhancement (PRE), after sunset. The pre-reversal enhancement consists of a rapid up shift of the F layer before the motion of the plasma be downward reverted. The main mechanism used to explain the development of the EPBs is the Rayleigh-Taylor (RT) instability. According to the theory, the RT growth rate is inversely proportional to the collision frequency between the neutral and ionic particles and it is proportional to the plasma density gradient. Thus, when the PRE is strong, it becomes more probable for EPBs occur.



In addition, the RT instability process needs a seeding mechanism, which has been largely studied in the last decades. Some researchers have pointed out gravity waves as seeding to the EPB (e.g., Fritts et al., 2008; Abdu et al., 2009; Takahashi et al., 2009; Taori et al., 2011; Paulino et al., 2011). Other studies have marked the dynamics of post sunset vortex and PRE dynamics as enough to the EPB origin (e.g., Kudeki and Bhattacharyya, 1999; Kudeki et al., 2007; Eccles et al., 2015; Tsunoda et al., 2018; Huang, 2018). The thermospheric neutral wind system and the associated electrodynamics have also been proposed as sufficient to the EPB appearance as well (e.g., Saito and Maruyama, 2009). Influences of magnetic storms and large scale waves have also been reported as important mechanism to the day-to-day variability of EPBs (e.g., Abalde et al., 2009; Huang et al., 2013).

Actually, observations have shown that there is a strong day-to-day variability of the EPB occurrence and development (e.g., Carter et al., 2014; Abdu, 2019) and it is a topic of current research. There is evidence of planetary waves acting in the neutral winds and consequently changing the background condition of the atmosphere (e.g., Forbes, 1996; Takahashi et al., 2006; Abdu and Brum, 2009; Chang et al., 2010; Zhu et al., 2017).

Stening and Fejer (2001) published the first work proposing the influence of lunar tides in the probability of occurrence of EPBs. It is well known that the main component of the lunar tides has a semimonthly oscillations. Based on these factors, the present work shows that there are semimonthly oscillations in the EPB, Plumes and Bottom Type Spread-F start time in different epochs of observations. Besides, these oscillations follow the Moon phases. These results can indicate strong evidences of the lunar semidiurnal tide modulating the wind system in the F region and consequently it is driving the time of generation of Spread-F.

## 2 Data Analysis

Airglow measurements of the OI 630.0 nm (OI6300) have been recorded at São João do Cariri (7.4°S, 36.5°W) since September 2000. In this investigation data from September 2000 to December 2010 were used, which corresponds to the first generation of the all sky imager deployed in this observatory.

The all sky imager is composed by a fish eye lens, a telecentric set of lens, a filter wheel, a set of lens to reconstruct the image, a Charge Coupled Device (CCD) chip and a cooling system. This instrument has a field of view of 180° of the sky. Further details of this imager have been published elsewhere (e.g., Paulino et al., 2016). Airglow images of the OI6300 were taken by about 15 days around the New Moon with integration time of 90 s. Depending on the mode of operation, images can have 2-4 min of temporal resolution. The start and end times can be extracted directly from the image header after observing the appearance or disappearance of the structures. The start time was defined as the time when the plasma bubbles appeared in the images. It generally occurs in the Northwest part of the images. After that, the plasma bubbles start their development and dynamics.

Figure 1 shows an example of the determination of the start time of EPBs on 27 January 2001. The supplementary short movie can help one to identify the time, in which the plasma bubbles start to extend to the southern part of the images.

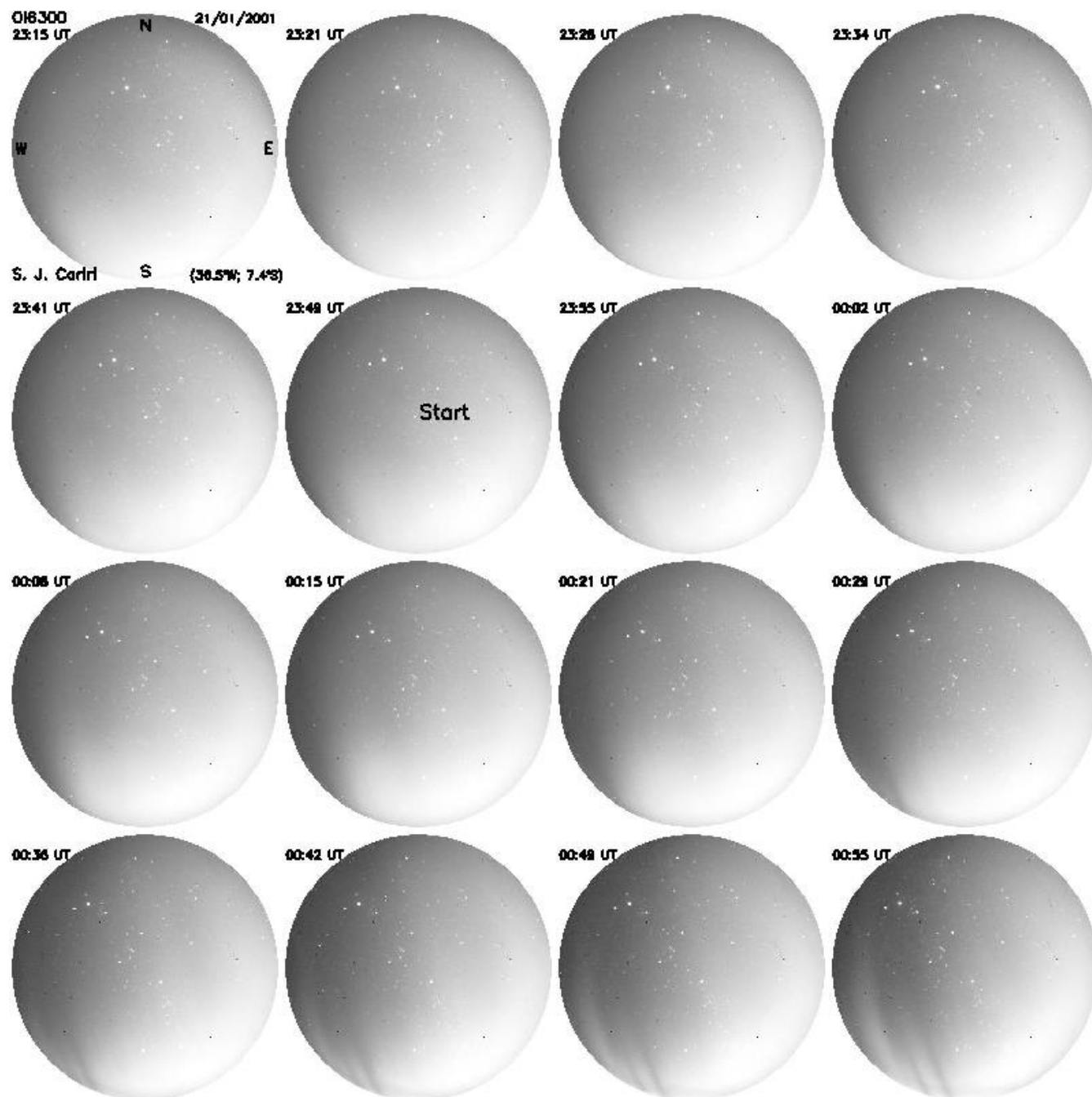


**Figure 1.** Sequence of OI6300 airglow images observed in São João do Cariri on 27 January 2001. One can observe the start time of the EPB on this night.

Corroborative data from a coherent VHF backscatter radar deployed at São Luís (2.6°S, 44.2°W) were also used to identify the start time of plume and bottom type spread F (BTSPF) structures. The data ranged from 02 September 2001 to 31 December



2008. The VHF coherent radar of São Luís operates at 30 MHz with a power peak of 4 kW. It has antenna half-power-full-beam-width of  $10^\circ$  and inter-pulse-period of 9.34 ms. The coverage in altitude of 87.5 to 1267 km and velocity of  $\pm 250 \text{ ms}^{-1}$ . The altitude resolution is 2.5 km and noise band width of 120 kHz. These characteristics allow to observe irregularities of 5 m in the ionosphere. Further technical details of the São Luís' radar can be found in de Paula and Hysell (2004) and Rodrigues et al. (2008).

Start time of Plume and BTSF were defined in Cueva et al. (2013). Those parameters correspond to the exact time of appearance of plumes and BTSFs in the range time integration (RTI) maps. The temporal resolution of the start time of the spread-F calculated in the RTI maps were 12 min.

### 3 Results and Discussion

10 Figure 2(a) shows the evolution of start time of the EPBs observed in September 2003 over São João do Cariri. The solid line represents the best fit for a periodicity of 14.5 days, the stars correspond to the exact time in which the plasma bubble appeared in the OI6300 images and the filled circle shows the New Moon time. In this case, one can see a good agreements of the fit line with the observation during a half cycle of the oscillation. The amplitude of this oscillation was calculated from the fitting as  $\sim 52$  min, i.e., there was a difference of  $\sim 52$  min in the start time of EPBs along the observed nights.

15 Figure 2(b) shows the best fit 14.5 days oscillation in the start time of EPBs observed from the later September to early October 2005. For the whole period of airglow observation, it was the best case study observed because it covers a full circle of the oscillation. There was an amplitude of  $\sim 37$  min and the position of the New Moon was observed on 03 October 2005. The predominance of this oscillation persists up to November 2005 as shown in Figure 2(c) with higher amplitude  $\sim 70$  min.

Similar results to September 2003 and November 2005 were found in January 2008 as one can see in Figure 2(d), inclusive  
20 the position of the New Moon in the cycle. The estimated amplitude was  $\sim 45$  min.

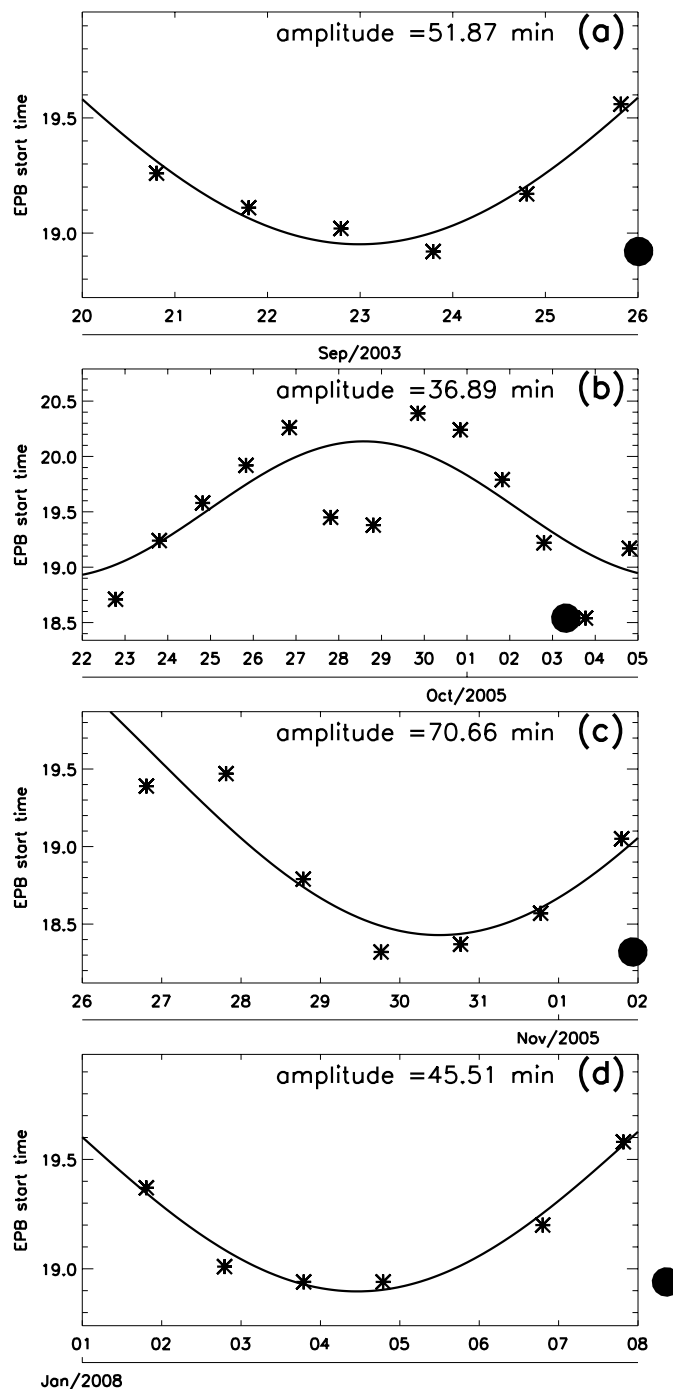


**Figure 2.** Start time of plasma bubble (stars) as function of time. Solid line represents the best fit to a sinusoidal oscillation with period of 14.5 days. The respective amplitudes are shown on the middle top of the panels. Panel (a) shows the results for September 2003. Panel (b) shows the results for September - October 2005. Panel (c) shows the results for October-November 2005. Panel (d) shows the results for January 2008. Filled circles indicate the New Moons.



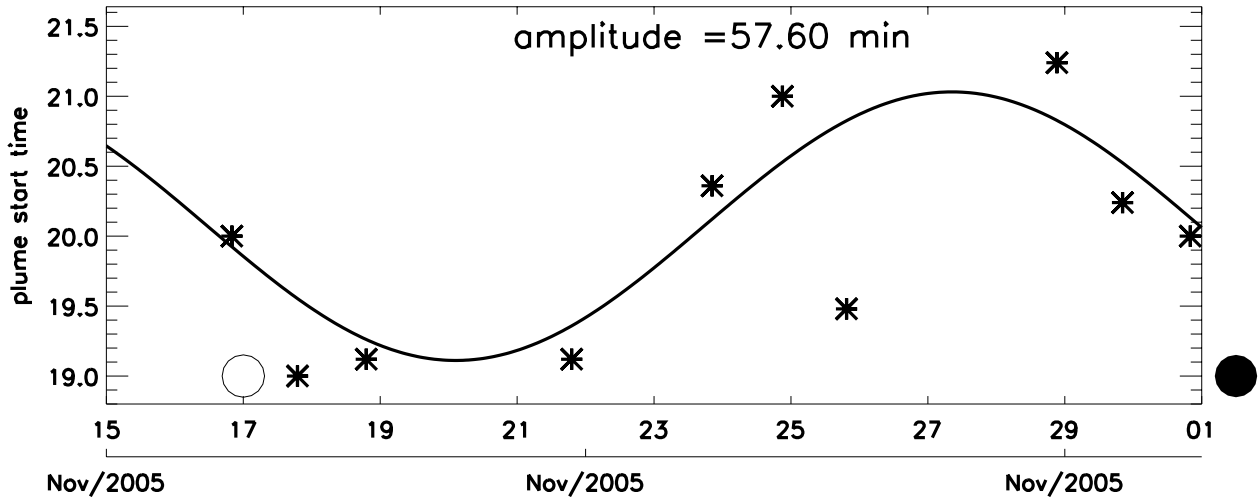
The results from Figure 2 indicate that the start time of EPBs was modulated by a semimonthly oscillation. Besides the results shown here, in other period of observation there were observed a tendency of the start time following this periodicities. However, only few days, less than a half month, were observed and those results are not shown here. The present work concentrate the discussion on the cases in which, a half cycle could be observed. Semimonthly oscillations well known in the atmosphere are: (1) Quasi 16 days planetary waves and (2) Lunar semidiurnal tide.

Simulations have shown that the 16d planetary waves (PWs) have large amplitudes in the winter hemisphere at the lower levels of the atmosphere and high latitudes, but above the mesosphere there is a penetration of this wave to the summer hemisphere, which allows it to be observed in both hemispheres including in the equatorial region (Miyoshi, 1999). Forbes and Leveroni (1992) have pointed out that 16d oscillation in the E and F-region could be connected by the upward propagation of Rossby wave from the winter stratosphere. Although the 16d PW have a well defined seasonality in the lower atmosphere, according to the simulations, in the upper atmosphere the presence of this oscillation has been predicted to be more spread along the year (Miyoshi, 1999). It is also important to mention that the 16d oscillations were observed in the mesosphere and lower thermosphere from 85 to 100 km altitude in the equatorial region in the zonal wind during the period around the September equinox and solstices of 1994 (Luo et al., 2002), which coincides to the periods of observation of the present results.

Lunar semidiurnal tides have been pointed out as important factor to the appearance and the start time of EPBs. The main reason for the influence of the Lunar tides in the EPB variability is the capability of the lunar tides propagate upward to high levels of the atmosphere and consequently it can affect the pre-reversal enhancement (PRE) amplitude and time (Stening and Fejer, 2001). Another factor to be considered is the moon phase (New Moon) that coincides to zero position of the oscillation for all observed cases, including the case studies observed from the coherent backscatter radar that will be shown ahead. The real mechanism that allows the lunar tides to act in the PRE is not well defined, but some works have pointed out as either the direct propagation to the bottom side of ionospheric F region (e.g., Evans, 1978; Forbes, 1982) or coupling of the E region dynamo to the F region (e.g., Immel et al., 2009; Eccles et al., 2011).

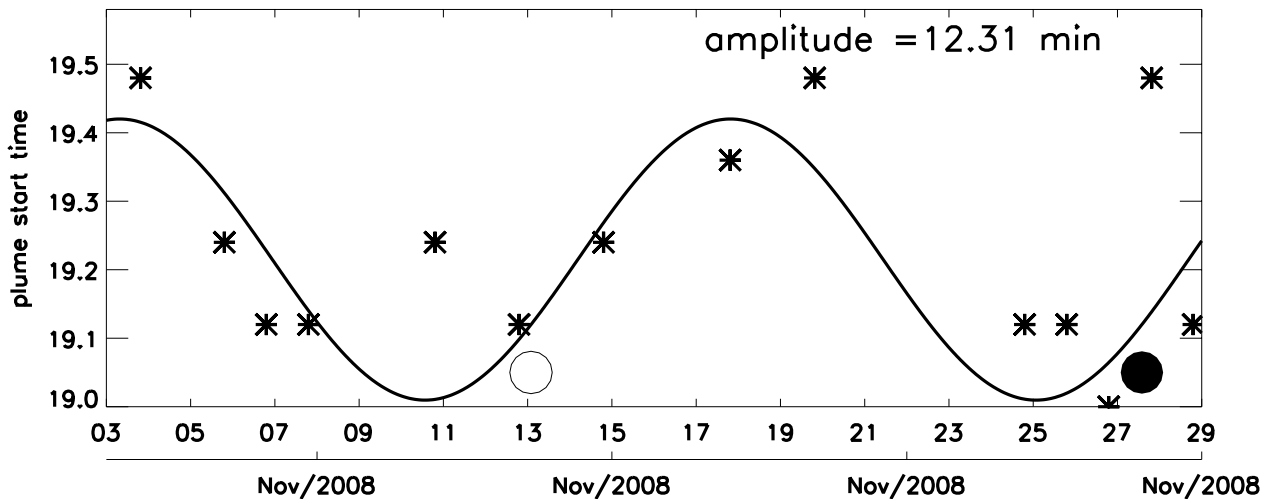
In order to corroborate the present results, data from the backscatter radar deployed in São Luís have been used to investigate the start time of the bottom type spread-F (BTSEF) and plumes. The main goal of these analysis is trying to observe more than one cycle of the semimonthly oscillation in the start time of spread-F, since the radar was operating continuously and does not depend on tropospheric weather conditions.

Figure 3 shows a complete cycle of 14.5 days in the start time of plume observed on November 2005, which coincide with the same period of observation of EPBs in the airglow images. For this case, an amplitude of  $\sim 1$  hour was observed.



**Figure 3.** Same as Figure 2, but for start time of plumes. Open circles indicate the Full Moon.

Figure 4 shows the start time evolution of the bottom type spread-F in November 2008, one can observe two complete cycles of the start time of the BTSF fitting a semi-month oscillation with an amplitude of  $\sim 12$  min.



**Figure 4.** Same as Figure 3, but for start time of bottom type spread-F.

Figures 3 and 4 show that the spread-F structures can be controlled by the semimonthly oscillation. However, the strong day-to-day variability of the spread-F does not allow to observe this signature always. Another difficulty in the radar data analysis was the algorithm does not give an exact start time of the oscillation, i.e., there was a temporal resolution of 15 min in this determination.



#### 4 Summary

Using almost one solar cycle of data from OI630 airglow images and range time integration maps from a backscatter radar in the equatorial region over Brazil, semimonthly oscillations in the start time of spread-F (EPBs, BTSF and Plumes) were observed and the results are summarized as follow:

- 5 – Four periods of airglow observation showed amplitudes higher than 36 min in the start time of EPBs for 14.5 days oscillation, three periods of observations (September 2003, October 2005 and January 2008) revealed good fit for half cycle and the another case (September 2005) showed and complete cycle;
- Two complete cycles of 14.5 days with amplitude of  $\sim 12$  min were observed in the bottom type spread-F in November 2008;
- 10 – Plumes observed in the RTI data showed a 14.5 cycle oscillation with amplitude of 1 hour in the start time of plumes during November 2005;

The present results indicate that one semimonthly dynamical structure can control either the start time or the amplitude of the PRE that can consequently produce Spread-F. These results must contribute to understanding the day-to-day variability of equatorial spread-F. However, the results shows that besides the semimonthly oscillations, other phenomena are important to the day-to-day variability occurrence of EPBs since this oscillations is not dominant in the whole period of observation. Regarding to the agents that are causing this oscillation, further investigation are necessary and they are out of the scope of this work. Lunar semidiurnal tides, which have semimonthly period of oscillation have been pointed out as a likely agent to produce this kind of oscillation in the start time of Spread-F. Besides, we have discussed the importance of 16d PWs that must be further investigated before being neglected.

20 *Data availability.* All sky image data can be requested from either the Aerolume (UFCEG) or Lume (INPE) Groups to the e-mail address to the first author of the manuscript. RTI maps can be requested from the Dr. Ricardo Y. C. Cueva ([navivacu@gmail.com](mailto:navivacu@gmail.com)).

*Author contributions.* IP has written the manuscript and made most of the airglow analysis. ARP has discussed the semimonthly oscillation due to lunar tides and 16d planetary waves. RYCC has calculated the start time of bottom type spread-F and plumes and provide technical information about the coherent radar. EA-Y has reduced the whole image data calculating the start time of EPBs. RAB has contributed to run the experiments in São João do Cariri and help with the analysis. HT has contributed to the discussion of 16d oscillation. AFM has provide some computing codes to work with the OI6300 airglow images.

*Competing interests.* The authors declare that they do not have competing interests;





*Acknowledgements.* I. Paulino thanks to Conselho Nacional de Desenvolvimento Científico e Tecnológico (CNPq) for the financial support (303511/2017-6). A. R. Paulino thanks to the Coordenação de Aperfeiçoamento de Pessoal de Nível Superior (CAPES) for the scholarship and CNPq by the grants ().



## References

- Abalde, J. R., Sahai, Y., Fagundes, P. R., Becker-Guedes, F., Bittencourt, J. A., Pillat, V. G., Lima, W. L. C., Candido, C. M. N., and de Freitas, T. F.: Day-to-day variability in the development of plasma bubbles associated with geomagnetic disturbances, *Journal of Geophysical Research: Space Physics*, 114, <https://doi.org/10.1029/2008JA013788>, 2009.
- 5 Abdu, M. A.: Day-to-day and short-term variabilities in the equatorial plasma bubble/spread F irregularity seeding and development, *Progress in Earth and Planetary Science*, 6, 11, <https://doi.org/10.1186/s40645-019-0258-1>, 2019.
- Abdu, M. A. and Brum, C. G. M.: Electrodynamics of the vertical coupling processes in the atmosphere-ionosphere system of the low latitude region, *Earth, Planets and Space*, 61, 385–395, <https://doi.org/10.1186/BF03353156>, 2009.
- Abdu, M. A., Alam Kherani, E., Batista, I. S., de Paula, E. R., Fritts, D. C., and Sobral, J. H. A.: Gravity wave initiation of equatorial  
10 spread F/plasma bubble irregularities based on observational data from the SpreadFEx campaign, *Annales Geophysicae*, 27, 2607–2622, <https://doi.org/10.5194/angeo-27-2607-2009>, 2009.
- Carter, B. A., Yizengaw, E., Retterer, J. M., Francis, M., Terkildsen, M., Marshall, R., Norman, R., and Zhang, K.: An analysis of the quiet time day-to-day variability in the formation of postsunset equatorial plasma bubbles in the Southeast Asian region, *Journal of Geophysical Research: Space Physics*, 119, 3206–3223, <https://doi.org/10.1002/2013JA019570>, 2014.
- 15 Chang, L. C., Palo, S. E., Liu, H.-L., Fang, T.-W., and Lin, C. S.: Response of the thermosphere and ionosphere to an ultra fast Kelvin wave, *Journal of Geophysical Research: Space Physics*, 115, <https://doi.org/10.1029/2010JA015453>, 2010.
- Cueva, R. Y. C., de Paula, E. R., and Kherani, A. E.: Statistical analysis of radar observed F region irregularities from three longitudinal sectors, *Annales Geophysicae*, 31, 2137–2146, <https://doi.org/10.5194/angeo-31-2137-2013>, 2013.
- de Paula, E. R. and Hysell, D. L.: The São Luís 30 MHz coherent scatter ionospheric radar: System description and initial results, *Radio  
20 Science*, 39, <https://doi.org/10.1029/2003RS002914>, 2004.
- Eccles, J. V., St. Maurice, J. P., and Schunk, R. W.: Mechanisms underlying the prereversal enhancement of the vertical plasma drift in the low-latitude ionosphere, *Journal of Geophysical Research: Space Physics*, 120, 4950–4970, <https://doi.org/10.1002/2014JA020664>, 2015.
- Eccles, V., Rice, D. D., Sojka, J. J., Valladares, C. E., Bullett, T., and Chau, J. L.: Lunar atmospheric tidal effects in the plasma drifts observed by the Low-Latitude Ionospheric Sensor Network, *Journal of Geophysical Research: Space Physics*, 116,  
25 <https://doi.org/10.1029/2010JA016282>, 2011.
- Evans, J. V.: A note on lunar tides in the ionosphere, *Journal of Geophysical Research: Space Physics*, 83, 1647–1652, <https://doi.org/10.1029/JA083iA04p01647>, 1978.
- Forbes, J. M.: Atmospheric tide: 2. The solar and lunar semidiurnal components, *Journal of Geophysical Research: Space Physics*, 87, 5241–5252, <https://doi.org/10.1029/JA087iA07p05241>, 1982.
- 30 Forbes, J. M.: Planetary Waves in the Thermosphere-Ionosphere System, *Journal of geomagnetism and geoelectricity*, 48, 91–98, <https://doi.org/10.5636/jgg.48.91>, 1996.
- Forbes, J. M. and Leveroni, S.: Quasi 16-day oscillation in the ionosphere, *Geophysical Research Letters*, 19, 981–984, <https://doi.org/10.1029/92GL00399>, 1992.
- Fritts, D. C., Vadas, S. L., Riggan, D. M., Abdu, M. A., Batista, I. S., Takahashi, H., Medeiros, A., Kamalabadi, F., Liu, H.-L., Fejer, B. G., and  
35 Taylor, M. J.: Gravity wave and tidal influences on equatorial spread F based on observations during the Spread F Experiment (SpreadFEx), *Annales Geophysicae*, 26, 3235–3252, <https://doi.org/10.5194/angeo-26-3235-2008>, <https://www.ann-geophys.net/26/3235/2008/>, 2008.



- Huang, C.-S.: Effects of the postsunset vertical plasma drift on the generation of equatorial spread F, *Progress in Earth and Planetary Science*, 5, 3, <https://doi.org/10.1186/s40645-017-0155-4>, 2018.
- Huang, C.-S., de La Beaujardière, O., Roddy, P. A., Hunton, D. E., Ballenthin, J. O., Hairston, M. R., and Pfaff, R. F.: Large-scale quasiperiodic plasma bubbles: C/NOFS observations and causal mechanism, *Journal of Geophysical Research: Space Physics*, 118, 3602–3612, <https://doi.org/10.1002/jgra.50338>, 2013.
- 5  
Immel, T. J., England, S. L., Zhang, X., Forbes, J. M., and DeMajistre, R.: Upward propagating tidal effects across the E- and F-regions of the ionosphere, *Earth, Planets and Space*, 61, 505–512, <https://doi.org/10.1186/BF03353167>, 2009.
- Kudeki, E. and Bhattacharyya, S.: Postsunset vortex in equatorial F-region plasma drifts and implications for bottomside spread-F, *Journal of Geophysical Research: Space Physics*, 104, 28 163–28 170, <https://doi.org/10.1029/1998JA900111>, 1999.
- 10  
Kudeki, E., Akgiray, A., Milla, M., Chau, J. L., and Hysell, D. L.: Equatorial spread-F initiation: Post-sunset vortex, thermospheric winds, gravity waves, *Journal of Atmospheric and Solar-Terrestrial Physics*, 69, 2416 – 2427, <https://doi.org/https://doi.org/10.1016/j.jastp.2007.04.012>, vertical Coupling in the Atmosphere/Ionosphere System, 2007.
- Luo, Y., Manson, A. H., Meek, C. E., Meyer, C. K., Burrage, M. D., Fritts, D. C., Hall, C. M., Hocking, W. K., MacDougall, J., Riggan, D. M., and Vincent, R. A.: The 16-day planetary waves: multi-MF radar observations from the arctic to equator and comparisons with the HRDI measurements and the GSWM modelling results, *Annales Geophysicae*, 20, 691–709, <https://doi.org/10.5194/angeo-20-691-2002>, <https://www.ann-geophys.net/20/691/2002/>, 2002.
- 15  
Miyoshi, Y.: Numerical simulation of the 5-day and 16-day waves in the mesopause region, *Earth, Planets and Space*, 51, 763–772, <https://doi.org/10.1186/BF03353235>, 1999.
- Paulino, I., Takahashi, H., Medeiros, A., Wrasse, C., Buriti, R., Sobral, J., and Gobbi, D.: Mesospheric gravity waves and ionospheric plasma bubbles observed during the COPEX campaign, *Journal of Atmospheric and Solar-Terrestrial Physics*, 73, 1575 – 1580, <https://doi.org/https://doi.org/10.1016/j.jastp.2010.12.004>, influence of Solar Activity on Interplanetary and Geophysical Phenomena, 2011.
- 20  
Paulino, I., Medeiros, A. F., Vadas, S. L., Wrasse, C. M., Takahashi, H., Buriti, R. A., Leite, D., Filgueira, S., Bageston, J. V., Sobral, J. H. A., and Gobbi, D.: Periodic waves in the lower thermosphere observed by OI630 nm airglow images, *Annales Geophysicae*, 34, 293–301, <https://doi.org/10.5194/angeo-34-293-2016>, 2016.
- 25  
Rodrigues, F. S., Hysell, D. L., and de Paula, E. R.: Coherent backscatter radar imaging in Brazil: large-scale waves in the bottomside F-region at the onset of equatorial spread F, *Annales Geophysicae*, 26, 3355–3364, <https://doi.org/10.5194/angeo-26-3355-2008>, 2008.
- Saito, S. and Maruyama, T.: Effects of transequatorial thermospheric wind on plasma bubble occurrences, *Journal of the National Institute of Information and Communications Technology*, 56, 257–266, 2009.
- 30  
Stening, R. J. and Fejer, B. G.: Lunar tide in the equatorial F region vertical ion drift velocity, *Journal of Geophysical Research: Space Physics*, 106, 221–226, <https://doi.org/10.1029/2000JA000175>, 2001.
- Takahashi, H., Wrasse, C. M., Pancheva, D., Abdu, M. A., Batista, I. S., Lima, L. M., Batista, P. P., Clemesha, B. R., and Shiokawa, K.: Signatures of 3-6 day planetary waves in the equatorial mesosphere and ionosphere, *Annales Geophysicae*, 24, 3343–3350, <https://doi.org/10.5194/angeo-24-3343-2006>, 2006.
- 35  
Takahashi, H., Taylor, M. J., Pautet, P.-D., Medeiros, A. F., Gobbi, D., Wrasse, C. M., Fechine, J., Abdu, M. A., Batista, I. S., Paula, E., Sobral, J. H. A., Arruda, D., Vadas, S. L., Sabbas, F. S., and Fritts, D. C.: Simultaneous observation of ionospheric plasma bubbles and mesospheric gravity waves during the SpreadFEx Campaign, *Annales Geophysicae*, 27, 1477–1487, <https://doi.org/10.5194/angeo-27-1477-2009>, <https://www.ann-geophys.net/27/1477/2009/>, 2009.



Taori, A., Patra, A. K., and Joshi, L. M.: Gravity wave seeding of equatorial plasma bubbles: An investigation with simultaneous F region, E region, and middle atmospheric measurements, *Journal of Geophysical Research: Space Physics*, 116, <https://doi.org/10.1029/2010JA016229>, 2011.

5 Tsunoda, R. T., Saito, S., and Nguyen, T. T.: Post-sunset rise of equatorial F layer—or upwelling growth?, *Progress in Earth and Planetary Science*, 5, 22, <https://doi.org/10.1186/s40645-018-0179-4>, 2018.

Zhu, Z., Luo, W., Lan, J., and Chang, S.: Features of 3–7-day planetary-wave-type oscillations in F-layer vertical drift and equatorial spread F observed over two low latitude stations in China, *Annales Geophysicae*, 35, 763–776, <https://doi.org/10.5194/angeo-35-763-2017>, 2017.